Search for Light Neutral Bosons in The TREK/E36 Experiment at J-PARC

Dongwi H. Dongwi (on behalf of the TREK/E36 Collaboration)
7000 East Ave., Livermore, CA 94550-9234
E-mail: dongwi1@llnl.gov

Abstract. The Standard Model (SM) represents our best description of the subatomic world and has been very successful in explaining how elementary particles interact under the influence of the fundamental forces. Despite its far reaching success in describing the building blocks of matter, the SM is still incomplete; falling short to explain dark matter, baryogenesis, neutrino masses and much more. The E36 experiment conducted at J-PARC in Japan, allows for sensitivity to search for light $U(1)$ gauge bosons, in the muonic K^+ decay channel. Such $U(1)$ bosons could be associated with dark matter or explain established muon-related anomalies such as the muon $g-2$ value, and perhaps the proton radius puzzle. A realistic simulation study was employed for these rare searches in a mass range of 20 MeV to 100 MeV. Preliminary results of the upper limits for the A' branching ratio $\mathcal{B}r(A')$ extracted at 95% CL, will be presented.

1. Introduction

The primary goal of the TREK/E36 experiment was to provide a high precision electroweak measurement in order to test lepton universality, which is expressed as an identical coupling constant of the charged lepton family (e, μ, and τ). Lepton universality is a staple of the Standard Model (SM) and any violation of this would be clear evidence of New Physics (NP) beyond the SM. The ratio of the two-body K^+ decay widths, of R_K is very precise because to a first approximation the strong interaction dynamics cancel, leaving behind equation 1 [1, 2]

$$\begin{aligned} R_K^{SM} &= \frac{\Gamma(K^+ \to e^+\nu)}{\Gamma(K^+ \to \mu^+\nu)} \\ &= \frac{m_e^2}{m_\mu^2}\left(\frac{m_K^2 - m_e^2}{m_K^2 - m_\mu^2}\right)^2 (1+\delta_r) \\ &= (2.477 \pm 0.001) \times 10^{-5} \end{aligned} \tag{1}$$

here δ_r represents radiative corrections, detailed calculations of which were carried out in [3]. Thus the SM value for R_K^{SM} has been calculated to high accuracy ($\Delta R_K/R_K \sim 0.4 \times 10^{-4}$) thereby making it possible to search for NP effects by conducting a precise measurement of R_K [1].

Additionally, the TREK/E36 experiment is sensitive to searches for light neutral particles in exotic kaon decay modes of $K^+ \to \mu^+\nu A'$ and/or $K^+ \to \pi^+ A'$, followed by a prompt decay of $A' \to e^+e^-$. Here, the A' channel of interest is in the muonic K_μ decay, $K^+ \to \mu^+\nu A'$. This

A', often dubbed a dark photon, could also be construed as a light neutral $U(1)$ boson, and might be a hidden force carrier of the dark sector associated with dark matter [4]. An A' that is weakly coupled to the SM and is sufficiently light could decay into observable di-lepton pairs, electron-positron pairs, which can be used to reconstruct its invariant mass. Furthermore, the A' could help resolve, simultaneously, the proton radius puzzle and anomalous magnetic moment of the muon $g_\mu - 2$ [5–8]. Such hypothetic particles can also be conceived without violating existing constraints if they are fine-tuned and non-universally coupled [6–11]. In this case there would be a prediction of a strong observable signal in kaon decays, in particular in the calculable leptonic radiative mode $K^+ \to \mu^+\nu e^+e^-$ [7, 8].

1.1. Carlson-Rislow Model

One such model, that proposes observable signals in leptonic K^+ decays, is the Carlson-Rislow model [8], which introduces a pair of new particles with polar and axial vector couplings to protons and muons respectively, in order to explain the proton radius puzzle while also obeying the $(g-2)_\mu$ discrepancy. The coupling strength of polar vector was chosen to explain the proton radius puzzle. The axial vector coupling enters the expression for the anomalous magnetic moment with an opposite sign to the polar vector, and was fine tuned to explain the $(g-2)_\mu$ discrepancy [7]. Rare kaon decays provide a good laboratory to test NP explanations for the proton radius puzzle. Beranek and Vanderhaeghen [12] have calculated constraints that the dark photon via kinetic mixing as well as lepton universality violating couplings are expected to contribute to the $K^+ \to \mu^+\nu e^+e^-$ decay. Carlson and Rislow [7, 8] calculated their light neutral boson's contribution to the $K^+ \to \mu^+\nu e^+e^-$ amplitude by modifying the photon's propagator and charged fermion couplings as follows [8]

$$\frac{-i}{q^2} \to \frac{-i}{q^2 - m_{A'}^2 + i m_{A'}\Gamma}, \tag{2}$$

$$-ie\gamma^\nu \to \gamma^\nu \varepsilon (C_V(m_{A'}) + C_A(m_{A'})\gamma^5), \tag{3}$$

where $C_V(m_{A'})$ and $C_A(m_{A'})$ are the polar and axial vector couplings to muons calculated in [7]. The couplings $C_{V,A}$ were chosen so as to obtain an extra 310 μeV muonic hydrogen Lamb shift from an electrophobic spin-0 or spin-1 particle as described in [7]. Figure 1 shows the muonic kaon decay involving an A' $K^+ \to \mu^+\nu A'$ followed promptly by $A' \to e^+e^-$.

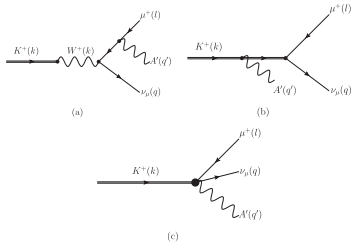

Figure 1: A' production amplitude. Feynman diagram showing the channel of interest $K^+ \to \mu^+\nu_\mu A'$ [12].

Carlson and Rislow have allowed for the possibility that the new particle has scalar and pseudoscalar couplings to muons and protons. They have modeled its contribution to the $K^+ \to \mu^+\nu e^+e^-$ amplitude by modifying the photons propagator as before and modifying the charged fermion couplings as [7]

$$-ie\gamma^{\mu} \rightarrow -i\varepsilon(C_S(m_{A'})) + iC_P(m_{A'}\gamma^5), \tag{4}$$

where $C_S(m_{A'})$ and $C_P(m_{A'})$ are the scalar and pseudoscalar couplings to muons as calculated in [7]. They have also calculated mass limits on polar and axial vector (as well as scalar and pseudoscalar) particles due to constraints placed by searches of muonic kaon decays $K^+ \rightarrow \mu X$. Their results are presented in figure 2. The solid curve in both figure 2 (a) and (b) is the result for a single particle with both polar (scalar) and axial vector (pseudoscalar) couplings. The horizontal line indicates the experimental limit, and ϕ can be taken to represent the A'.

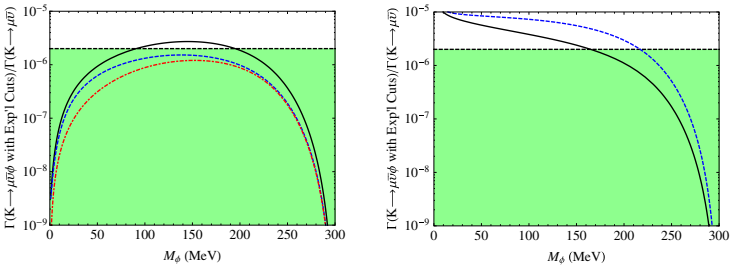

(a) (b)

Figure 2: Mass limits on particles with scalar and pseudoscalar (a), and polar and axial vector (b) couplings due to constraints placed by $K^+ \rightarrow \mu X$ searches. The solid curve is the result for a single particle with both polar (scalar) and axial vector (pseudoscalar) couplings. In (a) the contributions of scalar coupling is represented by the dashed curve and the dash-dotted curve represents the pseudoscalar coupling. In (b) the dashed curve is the result for separate polar and axial vector particles with equal masses, and in both (a) and (b) the green reqion represents the experimental limit (horizontal line) [7].

Carlson and Rislow have calculated the branching ratio $\mathcal{B}r(K^+ \rightarrow \mu^+\nu A')$ to be $\mathcal{O}(-5)$ for polar and axial vector couplings. Their prediction indicate that a strong signal peak over the SM background would be observed experimentally as shown in figure 3.

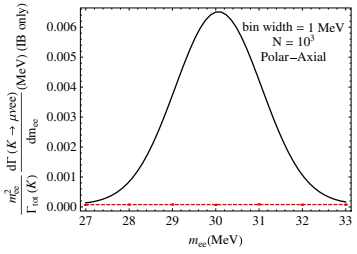

Figure 3: Strong signal to background prediction. The QED background prediction for $K^+ \rightarrow \mu^+\nu e^+e^-$ (red dashed curve) and the prediction with a 30 MeV lepton universality violating A' of the Carlson model [11].

Given the strong signal to background expectation of the Carlson model, the TREK/E36 experiment which is sensitive to light neutral bosons below 300 MeV would be able to test the efficacy of the Carlson model. The search would include a charged μ^+ that is detected in the spectrometer gap and two clusters in the CsI barrel from e^+-e^- pairs, from which a peak search will be conducted in the invariant mass spectrum M_{ee}.

2. Light Neutral Boson Search with the TREK/E36 Detecor Apparatus

TREK/E36 was set up and fully commissioned at the K1.1BR kaon beamline between the fall 2014 and spring 2015. Production data for the TREK/E36 experiment was completed by the end of 2015, which made use of an upgraded version of the KEK-PS E246 12-sector superconducting toroidal spectrometer used in a previous T-violation experiment via transverse muon polarization of muons in $K^+ \to \mu^+\nu\pi^0$ ($K_{\mu 3}$) decays at KEK [2, 13]. The schematic longitudinal and end views of the detector system are shown in figure 4.

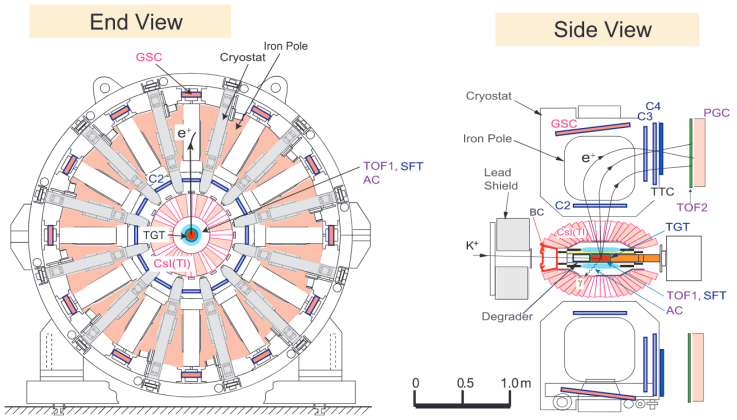

Figure 4: TREK/E36 apparatus. General cross-sectional and longitudinal views of the detector system.

The TREK/E36 apparatus upgrade from E-246 consisted of:

- scintillating fiber target used to stop the incoming kaon beam had a smaller diameter to minimize multiple scattering and energy loss of the outgoing decay particles [2]
- addition of Spiral Fiber Tracker [2, 14]
- redundancy in particle ID systems used to distinguish between e and μ with high efficiency and low misidentification probability [2]
- faster readout electronics of the CsI(Tl) calorimeter with a pile-up capable data acquisition system using FPGA based waveform digitization [2, 15].

The incoming K^+ was tagged with a Fitch Čerenkov detector [2], in order to distinguish it from a π^+, before stopping and decaying at rest in the active target, a matrix of 256 scintillating fibers oriented longitudinally along the beam, which determines the location of the kaon stop in the transverse plane. Surrounding the target was the a Spiral Fiber Tracker (SFT), which consisted of two pairs of fiber layers spiraling in *left/right* helicity and provided the z-coordinate of the of the outgoing decay particle(s) [14]. The target-SFT system was surrounded by 12 time-of-flight counter (TOF1) and 12 aerogel Čerenkov counters (AC) aligned with the 12 sectors of the toroidal spectrometer. This entire inner system is called the *Central Detector* system (CD).

A highly segmented and large acceptance CsI(Tl) calorimeter barrel which consisted of 768 crystal and covered about 75% of 4π [16] was used to identify and correct for structure dependent (SD) background events and also search for light neutral bosons A'. The calorimeter featured 12 holes (known as *muon holes*) aligned with the sectors of the spectrometer allowing for charged particles such as e^+, μ^+ and π^+ to be tracked through 1 of the 12 toroidal magnet gaps, and momentum analyzed with Multi-Wire Proportional Chambers (MWPC) C2, C3 and C4. The A' search necessitated a charged particle tracked in the gap that has a vertex originating within

the fiducial volume of the target (*good gap event*) and 2-clusters in the CsI calorimeter along with at least 3 TOF1 counters that registered a charged particle (ideally: e^+, e^- and a good gap μ^+). At the exit of each magnet gap were sets of fast scintillator detectors (TTC and TOF2) and lead glass counters (PGCs) [17] that provided both trigger signals and e^+/μ^+ particle ID. The full suite of particle ID systems and tracking can also be deployed to suppress background events in the invariant mass spectrum when performing the A' search.

3. CsI Analysis and A' Search Strategy

Calibration of the CsI barrel was carried with monochromatic $K_{\mu 2}$ energy. A cross check of the calibration was performed with the $K_{\pi 2}$ momentum pre-selection, and the associated 2-γ clusters as shown in figure 5.

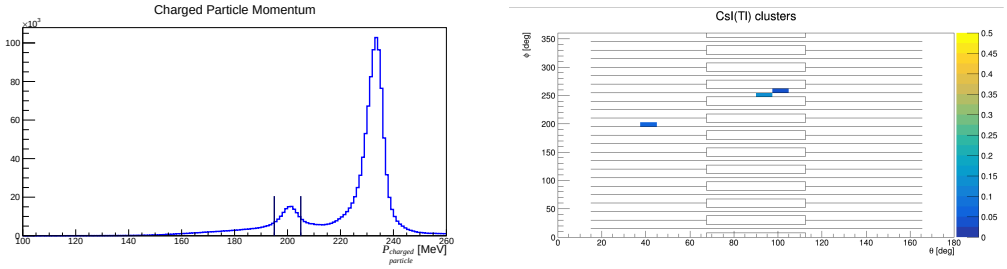

(a) (b)

Figure 5: Pre-selected $K_{\pi 2}$ cluster hits in the CsI calorimeter. $K_{\pi 2}$ momentum selection cut in (a), with black lines indicating the generous selection invterval. The CsI event viewer (b) showing a given cluster hit pattern.

Two photon cluster events in the CsI detector were used to reconstruct the invariant mass of the π^0, well as the total cluster energy. An energy-weighted centroid technique was employed for this reconstruction. Since the CsI(Tl) was operated with high hardware threshold ($\approx$ 20 MeV), only crystals with energies greater than 20 MeV participated for a given event. For this reason, single crystals were considered to be part of a cluster, namely a *single crystal cluster*.The reconstructed π^0 invariant mass from simulation (red) was observed to have a thinner peak compared to the data and a similar situation was also observed for the sum of the 2γ cluster energies, as seen in figure 6.

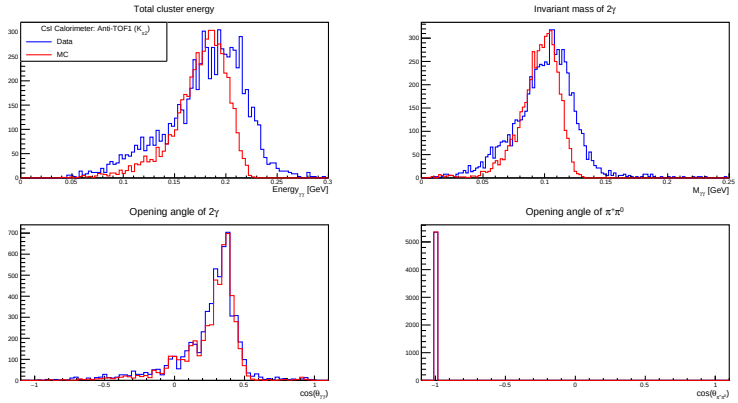

Figure 6: Plots of total energy, invariant mass of 2γ clusters, opening angle of 2γ's, $cos(\theta_{\gamma\gamma})$, and opening angle of $\pi^+\pi^0$ $cos(\theta_{\pi^+\pi^0}) \leq -.99$. Better agreement between data and simulation was achieved by requiring that only a single TOF1 has registered a hit per event.

3.1. A' Search Strategy

A necessary condition for the A' search is to have a so-called good gap event. This means that a charged particle has escaped from the openings in the CsI barrel, and had its momentum evaluated by the spectrometer magnet, and has registered hits in the ToF and C-detector elements. In the TREK/E36 experiment, theA' search was performed in the muonic kaon decay channel $K^+ \to \mu^+\nu A'$, followed by the prompt $A' \to e^+e^-$ decay. The trigger condition for the A' required a charged particle in the gap and 3 TOF1 counters that registered a hit. Ideally, one of the three TOF1 counters corresponds a tracked μ^+ while the other two register e^+ and e^-. The criteria for clusters in the calorimeter can be summarized as follows:

(i) good gap event, i.e. a charged particle has a track that originated in the target and was tracked by the three MWPCs,
(ii) momentum cut $p < 230$ MeV/c,
(iii) only two clusters were observed in the calorimeter,
(iv) 3 TOF1 counters with registered hits

The e^+-e^- pair would then go on to form two clusters in CsI calorimeter, which can be used to produce an invariant mass spectrum M_{ee}. A peak search over a continuous background is needed to determine if an A' signal is present. With this criteria in place, the search for A' proceeds as laid out in figure 7.

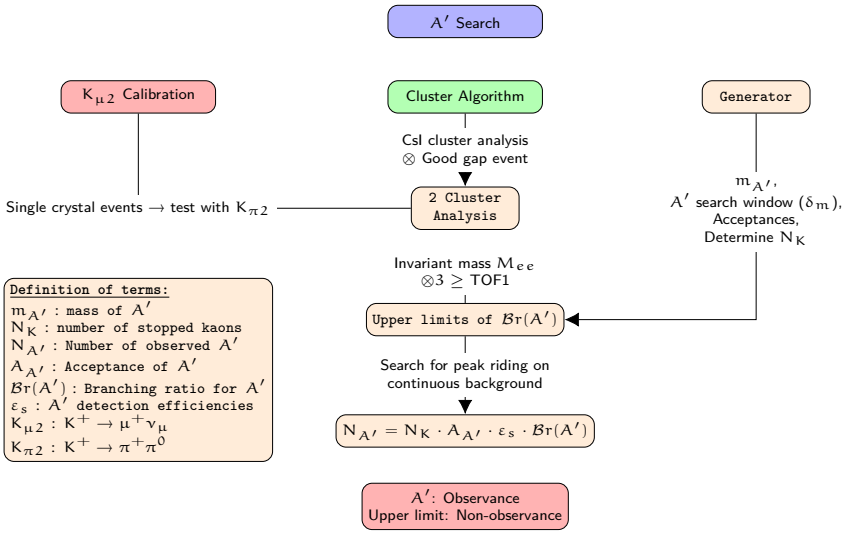

Figure 7: A' search strategy analysis flow schema, showing the combination of cluster analysis, *good gap* event, and upper limit at 95% CL.

4. Preliminary Upper Limit Extraction

Aforementioned, the A' signal search required a TOF1 multiplicity of 3 or greater, implying that three charged particles passed through the TOF1 counters. An additional cut on a good gap event where a charged particle registered hits in the tracking detectors C2, C3 and C4, was deployed provided that the track vertex lies within the fiducial volume of the target. A further endpoint momentum cut, shown in figure 8, was applied for the express purpose of suppressing the $K_{\mu 2}$ muons.

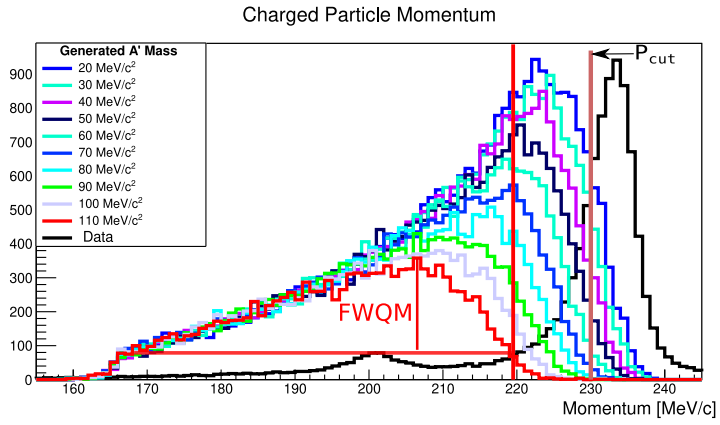

Figure 8: Endpoint momentum cut, with a hard cut placed at 230 MeV/c. A variable full-width at quarter max (FWQM) cut was employed iff less then the hard cut at 230 MeV/c.

Noticeable effects of these sequential background suppression cuts can be both summarize and observed in figure 9, by way of the invariant mass distributions. The blue histogram corresponds to all the events that have two clusters in the CsI and a charged particle in the gap. The grey, teal, violet, and dark colored histograms reflect the endpoint, M^2, and combined PID, cut respectively.

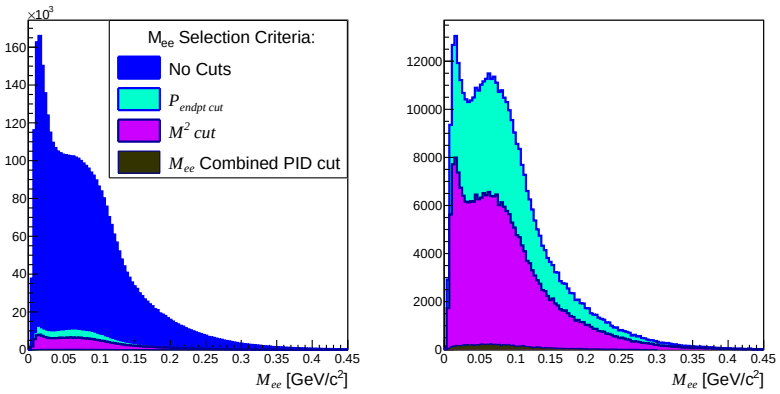

Figure 9: Invariant mass M_{ee} distributions under three cut conditions: good gap (blue); $K_{\pi 2}$ momentum region (green) and extra TOF1 (red).

The combined PID cut employs all the preceding cuts in addition to strict angular correlation between fired TOF1 counters and the corresponding CsI clusters. A fit to the M_{ee} for cuts of endpoint momentum cut in conjunction with M^2 cut, was performed and the results are show below in figure 10, with the residual, plotted in the panel below.

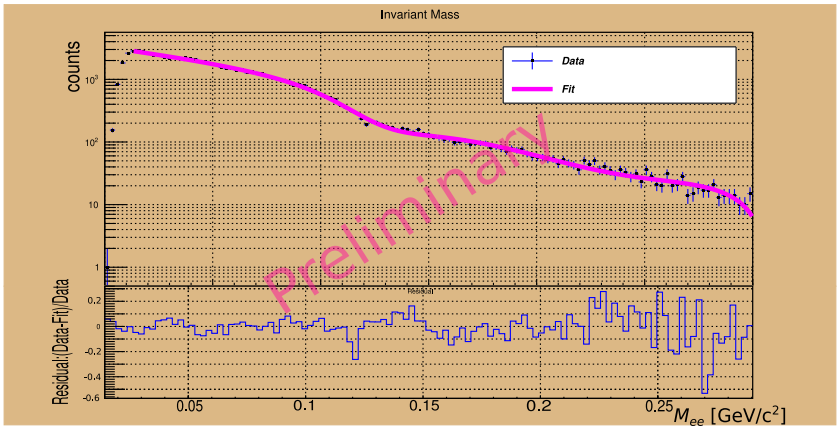

Figure 10: Invariant mass distribution with fit to data and residual is shown in the bottom plot.

The fit function from figure 10 and the total number of stopped kaons N_K were used to extract the upper limits. N_K, the total number of stopped K^+ in the fiducial region of the active target was computed as follows

$$N_K = \frac{N_{\mu 2}}{\mathcal{B}r(\mu 2) PS_{\mu 2} A_{\mu 2} LT_{\mu 2}} = 2.81 \times 10^9 \quad (5)$$

where $N_{\mu 2}$ is the number of tracked data candidates satisfying the $K_{\mu 2}$ decay momentum, $A_{\mu 2}$ is the acceptance of the $K_{\mu 2}$ muons evaluated with the MC simulations, $\mathcal{B}r(\mu 2)$ is the nominal branching ratio of the $K_{\mu 2}$ decay mode and $PS_{\mu 2} = 49$ and $LT_{\mu 2} = 1$ are the muon

prescale factor and livetime fraction respectively. Upper limits at 95% CL on the branching ratio of $Br(A')$ for each A' mass, corresponding to a 2σ limit of not observing the A', under the assumption that $Br(A' \to e^+e^-) = 1$ were computed using the relation

$$Br(A') < \frac{2\sqrt{N_{\mu\nu ee}}}{N_K A_{A'} \cdot LT}. \tag{6}$$

The invariant mass M_{ee} spectrum reflecting the background reduction as result of the endpoint momentum cut, M^2 and TOF1 ≥ 3 is shown in figure 11 (a). The with $\sim 20\%$ of data analysed, the upper limit was found to be at $\mathcal{O}(-6)$.

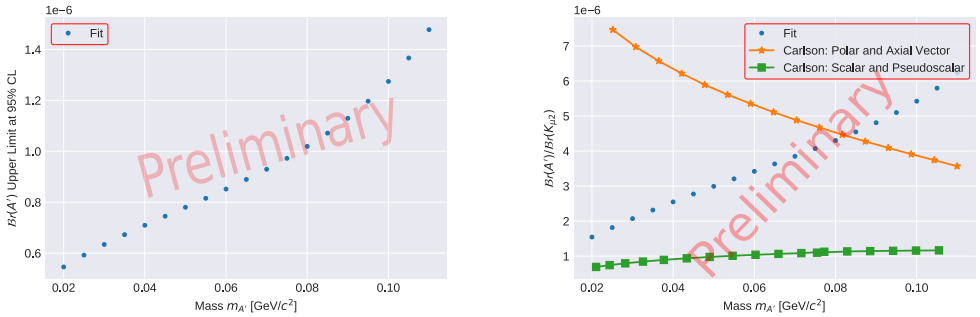

(a) (b)

Figure 11: Upper limit extraction (a) as a function of reconstructed A' mass. Data (blue) and theory mass limit comparisons (b) on particles with scalar and pseudoscalar (squares), and polar and axial vector (stars) couplings. Particles with both polar and axial vector coupling are excluded for masses below 0.08 GeV/c^2.

Experimental limits from the Carlson model for new light neutral bosons with polar (scalar) and axial vector (pseudoscalar) couplings are $\mathcal{O}(-6)$, see figure 2. Whereas figure 11 (b), shows the comparison between data and theory prediction of the mass limits on particles with scalar and pseudoscalar (green), and polar and axial vector (orange) couplings due to constraints placed by $K^+ \to \mu X$ searches [7]. A particle with both polar and axial vector coupling, is already excluded for masses below 0.08 GeV/c^2 with only $\sim 20\%$ of the data analysed. However, a single particle with both scalar and pseudoscalar coupling is not yet excluded. With further development in reducible background suppression, and more data analysis, we are hoping to enhance sensitivity and enhance experimental reach. Presently data with a combined PID cut have not yet been assessed and the AC cuts have not been applied for $e/\mu/\pi$ mis-identification suppression. This cut would serve further reduce the reducible background, and would enhance our sensitivity to particles with scalar and pseudoscalar couplings.

5. Preliminary Results and Outlook

The TREK/E36 experiment has completed its data-taking and has been decomissioned as of March 2016. A Geant4 and ROOT based MC, e36g4MC, was developed to assist with rare kaon decay searches for light neutral bosons. A search for the A' production in the $K^+ \to \mu^+\nu A'$, followed by the prompt decay of $A' \to e^+e^-$ along with a charged particle that was detected and tracked in the spectrometer gap, was performed using data from the TREK/E36 experiment. The sensitivity of TREK/E36 to A' production was evaluated via upper limits of the branching ratios $Br(A')$ as a function of $m_{A'}$ and found were to be $\mathcal{O}(-6)$, with about 20% of the data analyzed. The experimental limit from the Carlson model for a new

light neutral with polar (scalar) and axial vector (pseudoscalar) couplings are $\mathcal{O}(-6)$, see figure 2. Particles with both polar and axial vector coupling, is already excluded for masses below 0.08 GeV/c^2 with only $\sim 20\%$ of the data analysed. However, a single particle with both scalar and pseudoscalar coupling is not yet excluded. Finally, a fully digitized and realistic e36g4MC would be instrumental in further studies of light neutral bosons. A fully digitized e36g4MC would be essential in providing a realistic description of detector responses as well as a full reproduction of known SM backgrounds. As a result the e36g4MC would play a pivotal role in reducing the SM backgrounds and increase our sensitivity to A' production.

6. References

[1] Vincenzo Cirigliano and Ignasi Rosell. Two-loop effective theory analysis of pi(K) $\to$ e anti-nu/e [gamma] branching ratios. *Phys. Rev. Lett.*, 99:231801, 2007.
[2] C. Rangacharyulu, et al. J-PARC Experimental Proposal Measurement of $\Gamma(K^+ \to e^+)/\Gamma(K^+ \to \mu^+\nu)$ and Search for heavy sterile neutrinos using the TREK detector system.
[3] Vincenzo Cirigliano and Ignasi Rosell. $\pi/K \to e\overline{\nu}_e$ branching ratios to $\mathcal{O}(e^2p^4)$ in Chiral Perturbation Theory. *JHEP*, 10:005, 2007.
[4] James D. Bjorken, Rouven Essig, Philip Schuster, and Natalia Toro. New Fixed-Target Experiments to Search for Dark Gauge Forces. *Phys. Rev.*, D80:075018, 2009.
[5] David Tucker-Smith and Itay Yavin. Muonic hydrogen and MeV forces. *Phys. Rev. D*, 83:101702, 2011.
[6] Brian Batell, David McKeen, and Maxim Pospelov. New Parity-Violating Muonic Forces and the Proton Charge Radius. *Phys. Rev. Lett.*, 107:011803, 2011.
[7] Carl E. Carlson and Benjamin C. Rislow. New Physics and the Proton Radius Problem. *Phys. Rev.*, D86:035013, 2012.
[8] Carl E. Carlson and Benjamin C. Rislow. Constraints to new physics models for the proton charge radius puzzle from the decay $K^+ \to \mu^+ + \nu + e^- + e^+$. *Phys. Rev. D*, 89(3):035003, 2014.
[9] Tommi Alanne, Giorgio Arcadi, Florian Goertz, Valentin Tenorth, and Stefan Vogl. Model-independent constraints with extended dark matter EFT. 6 2020.
[10] Marco Fabbrichesi, Emidio Gabrielli, and Gaia Lanfranchi. The Dark Photon. 5 2020.
[11] Carl E. Carlson and Michael Freid. Extending theories on muon-specific interactions. *Phys. Rev. D*, 92(9):095024, 2015.
[12] T. Beranek and M. Vanderhaeghen. Constraints on the Dark Photon Parameter Space from Leptonic Rare Kaon Decays. *Phys. Rev.*, D87(1):015024, 2013.
[13] K. Paton, et al. Measurement of T-violation Transverse Muon Polarization in $K^+ \to \pi^0\mu^+\nu$ Decays.
[14] O. Mineev et al. The design and basic performance of a Spiral Fiber Tracker for the J-PARC E36 experiment. *Nucl. Instrum. Meth.*, A847:136–141, 2017.
[15] Youichi Igarashi and Masatoshi Saito. Waveform sampler module for j-parc trek experiment. In *Waveform sampler module for J-PARC TREK experiment*, pages 1376–1379, 2012.
[16] D. V. Dementev et al. CsI(Tl) photon detector with PIN photodiode readout for a $K_{\mu 3}$ T-violation experiment. *Nucl. Instrum. Meth.*, A440:151–171, 2000.
[17] Y. Miyazaki et al. Performance test of a lead-glass counter for the J-PARC E36 experiment. *Nucl. Instrum. Meth.*, A779:13–17, 2015.

7. Acknowledgements

This work is supported in part by NSERC and NRC in Canada, the KAKEN-HI Grants-in-Aid for Scientific Research in Japan, the DOE and NSF in the US, and in Russia by the Ministry of Science and Technology.
Prepared by LLNL under Contract DE-AC52–07NA23744.